INFLUENCE OF MILLING METHOD ON THE ELECTRICAL PROPERTIES OF 0.65PMN-0.35PT CERAMICS

Arjin Boonruang*, Piyalak Ngernchuklin, Saengdoen Daungdaw, and Chutima Eamchotchawalit

Received: August 22, 2012; Revised: January 23, 2013; Accepted: February 11, 2013

Abstract

Stoichiometric 0.65PMN-0.35PT ceramics have been fabricated from calcined powders, which were ground by 2 different milling methods, conventional ball milling and high energy ball milling. The milling conditions of both milling methods were identical. The results of the particle size distribution showed a submicron range after milling at 200 rpm for 16 h. The powders were pressed by hydraulic pressing and cold isostatic pressing. The fully dense samples with a relative density of 96% were obtained after sintering at 1100°C. Their electrical properties with respect to the milling methods were observed. It was found that the ceramics started with the calcined powder which was prepared by high energy ball milling had higher electrical properties than those of the ceramics which were started with the calcined powder which was prepared by conventional ball milling.

Keywords: High energy ball milling, conventional ball milling, hydraulic pressing, cold isostatic pressing, PMN-PT ceramic

Introduction

The lead magnesium niobate-lead titanate ($(1-x)Pb(Mg_{1/3}Nb_{2/3})O_{3-x}PbTiO_3$) (PMN-PT) system at the morphotropic phase boundary (x = 0.3-0.4) has tetragonal and rhombohedral phases leading to its high piezoelectric properties and dielectric constant which are comparable to or better than those of PZT-5H (Kelly *et al*., 1996; Kelly, 1998). Thus, PMN-PT has been an attractive material for electronic devices including ceramics, multilayer capacitors, piezoelectric actuators, and pyroelectric detectors. It is well known that the electrical properties of the ceramics are closely related to their powder preparation methods. Synthesis of ferroelectric powders has a significant role in defining the microstructure, electrical, and optical properties of the ferroelectric ceramics (Kong *et al*., 2008). The milling of the calcined materials plays an important role in powder preparation in order to obtain chemical and physical homogeneities (Haertling, 1999). It has been reported that the conventional ball milling method required high sintering temperatures resulting in higher lead loss from lead oxide (PbO) volatilities, thus worsening the micro-

Thailand Institute of Science and Technological Research, Techonopolis, Klong Luang, Pathumthani, 12120, Thailand. E-mail: arjin@tistr.or.th

* *Corresponding author*

structural and, subsequently, the electrical properties of ferroelectric materials (Kong *et al.*, 2008). A crucial parameter for good properties of the samples was to control the particle size distribution and homogeneity of the powders; thus milling of calcined powders could be used by the mechanochemical synthesis of the ceramic powders (Brankovic *et al.*, 2003). The mechanochemical process can provide better chemical mixing and produce smaller particle size materials, and thus it could enhance the electrical properties of the ceramics (Ng *et al.*, 2009). These reasons make them an alternative way to improve both the physical and electrical properties of ceramics at a lower sintering temperature. In this research, perovskite 0.65PMN-0.35PT ceramics from submicron powders synthesized via 2 different methods, a high-energy ball milling and a conventional ball milling, were prepared. The influence of the particle size distribution on the electrical and piezoelectric properties of ceramics at lower temperatures was observed and discussed.

Materials and Methods

In this research, the composition at morphologic phase boundary of the ceramics (0.65PMN-0.35PT) was prepared by the columbite method (Swart and Shrout, 1982). The precursor of magnesium niobate was synthesized from $((MgCO_3)4.Mg(OH)_2.5H_2O$, reagent grade, (Carlo Erba Reagenti SpA, Milan, Italy) and Nb_2O5 (99%, Merck KGaA, Darmstadt, Germany) in acetone by ball milling for 24 h, then calcined at 1000°C for 4 h. After that, the magnesium niobate precursor was mixed with PbO (99%, Kanto Chemical Co. Inc., Tokyo, Japan) and TiO_2 (99%, Honeywell Riedel-de Haen AG, Seelze, Germany). Excess PbO (0.5 wt%) was added to compensate for the lead loss. The mixture was ball milled in acetone for 24 h, then calcined at 900°C for 4 h. The calcined 0.65PMN-0.35PT powder was ground by high energy ball milling (HBM) which was carried out in a Fritsch Pulverisette 5 planetary high-energy ball milling system (Fritsch GmbH, Kastl, Germany) at room temperature. A 250 ml zirconia vial and alumina balls with 5 mm diameter were used. The conventional ball milling (CBM) was performed by using a 250 ml high density poly-ethylene bottle and 5 mm diameter alumina balls. Themilling conditions of both methods were shown in Table 1. The calcined powders were placed in a vial with isopropyl alcohol (IPA) 50 ml. The milling speed was controlled at approximately 200 rpm and the milling duration used was 16 h. The difference was that the HBM was applied by a non-continuous process (stopping every hour for 15 min), while the CBM was a continuous process.

Then, after drying, the powders were mixed with 6 wt% polyethylene glycol (binder) solution and sieved through 135 mesh. The green pellets were pressed into disks of 1.2 cm in diameter and a 0.1 cm thickness. All samples were heated at 550°C for 1 h to burn out the binder and were then sintered at 1100°C for 2 h.

The particle size distributions of the

Table 1. Milling conditions of HBM and CBM

Milling method	HBM	CBM
Batch size	250 ml	
Ball weight	330 g	
Milling media	5-mm Alumina balls	
Milling environment	Isopropanal (IPA)	
Jar rotation speed	200 rpm	
Milling time	16 h	
Milling condition	non-continuous	continuous

calcined powders prepared from HBM and CBM were evaluated by a particle size analyzer (Mastersizer 2000, Malvern Instruments Ltd., Malvern, UK). X-ray diffraction (XRD-6000, Shimadzu Corporation, Tokyo, Japan) with a Fe source (λ = 1.93 Å) was used to identify the phases of the sintered ceramics. The densities of the sintered pellets were determined by the Archimedes principle. The microstructure of the fracture and surface of the pellets were observed by Scanning Electron Microscopy (SEM) using a JSM-6340F JEOL Ltd., Tokyo, Japan).

Before the electrical measurements, the samples were polished to flat and parallel surfaces then electroded with silver paste by painting.

i) The piezoelectric PMN-PT samples were pooled in the silicone oil at 120°C and 25 kV/cm for 5 min. The piezoelectric coefficient (d_{33}) was determined with a Berlincourt Piezo d_{33} meter (Doon Ceratronics Pvt. Ltd., Uttarakhand, India).

ii) The dielectric constant (K) and the dissipation factor (tan δ) values were measured at 1 kHz with an impedance analyzer (4192A LF, Hewlett-Packard Company, Palo Alto, CA, USA) at room temperature.

Results and Discussion

Phase Analysis of the Calcined 0.65PMN-0.35PT Powders

Figure 1 shows the XRD patterns of the 0.65PMN-0.35PT calcined powders after the HBM and CBM methods. The XRD peaks demonstrated the PMN perovskite structure, which could be matched with the Joint Committee on Powder Diffraction Standards (JCPDS) file no. 81-861 and no observation of the secondary phase of pyrochlore. Moreover, it showed the k_α peak of the Fe source due to no filter being used in such Fe-target. The characteristic of the XRD peaks for both the calcined powders after HBM and CBM were sharp with distinctive diffractions, which was evidence that the complete PMN-PT crystalline structure was obtained.

Particle Analysis of the Calcined 0.65PMN-0.35PT Powders

The particle size distributions of the calcined powders before and after grinding by the HBM and CBM methods are displayed in Figure 2. It was observed that the mean particle

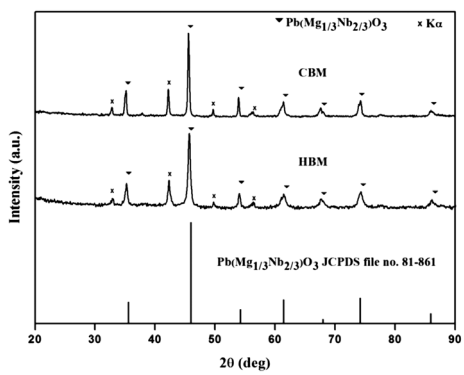

Figure 1. XRD patterns of the 0.65PMN-0.35PT calcined powders from HBM and CBM methods

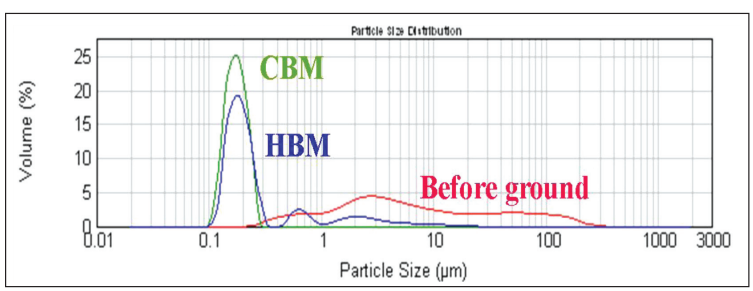

Figure 2. The particle size distribution of the calcined powders by High Energy Ball Mill (HBM) and Conventional Ball Mill (CBM)

sizes were decreased from 4.2 μm (before grinding) to 0.19 μm (after grinding by HBM) and 0.17 μm (after grinding by CBM). In addition, the powders from HBM had a trimodal size distribution with the majority peak of particle size at 0.19 μm associated with various sizes of 0.63 and 2.19 μm while the powder from CBM showed a monomodal size distribution of which the mean particle size was approximately 0.17 μm. The trimodal size distribution of HBM may be caused by the non-continuous milling process (20 min stopping in every hour) to prevent heat and the evaporation of the IPA solvent during the milling process.

The Powder Morphology

The powder morphology and agglomeration are investigated by SEM in Figure 3. It can be seen that the calcined powder ground with both HBM and CBM were similar and had an irregular shape. Besides, the powders of both methods had a nano-meter range grain size, this resulting in a high degree of agglomeration.

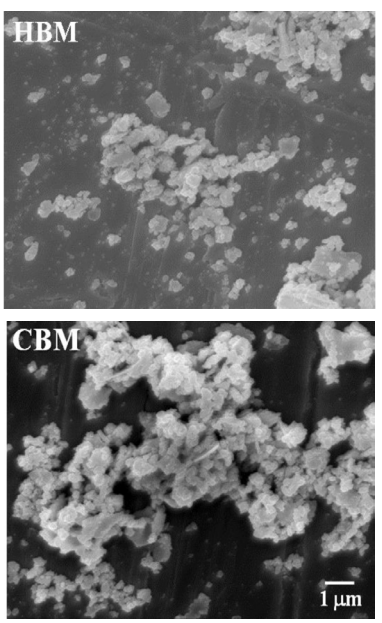

Figure 3. SEM of the 0.65PMN-0.35PT powders ground by High Energy Ball Mill (HBM) and Conventional Ball Mill (CBM)

Phase Analysis of the 0.65PMN-0.35PT Sintered Ceramics

Figure 4 presents the XRD patterns of the 0.65PMN-0.35PT sintered ceramics from the HBM and CBM calcined powders. The XRD pattern showed the pure phase of the PMN perovskite structure which matched with JCPDS file no. 81-861. It can be seen that there is no observation of a pyrochlore phase in both cases; it may be due to the excess of 0.5 wt% PbO that could prevent the PbO loss causing the formation of pyrochlore during the sintering step.

Microstructure of the 0.65PMN-0.35PT Sintered Ceramics

Figure 5 shows the surface (a and c) and fracture (b and d) of the sintered ceramics from the calcined powders which were ground via HBM and CBM. Both samples showed dense microstructure with a relative density of 96-97%. The average grain size of both samples was similar. The grain size of ceramics from the HBM- and CBM-derived powder was in the range of 0.5-4 μm. Moreover, a combination of SEM and energy-dispersive X-ray techniques had revealed an unreacted precursor MgO phase. It was interesting to note that the nano-scale MgO inclusions were also found in both cases and always investigated in the columbite route. This result was in agreement with Costa *et al*. (2001) and Wongmaneerung *et al*. (2006), although

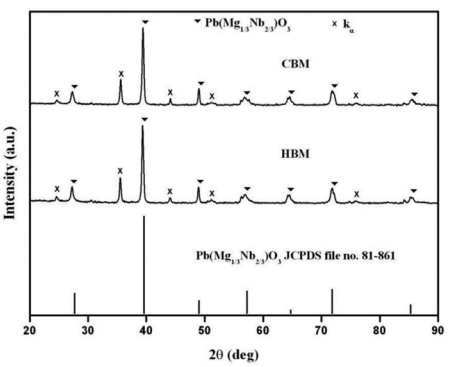

Figure 4. XRD patterns of the 0.65PMN-0.35PT sintered ceramics (1100°C/2h) from HBM and CBM calcined powders

it could not detected by XRD due to the limitation of the XRD technique which required at least 5 wt% of the component (Klug and Alexander, 1974; Wongmaneerung *et al*., 2006). In addition, both sintered ceramics had abnormal grain growth (Figure 5(a) and 5(c)). This type of grain was activated by the grain boundary mobility due to the existence of a PbO-rich liquid phase during the long thermal treatment (Gorzkowshi *et al*., 2006; Amorin *et al*., 2008). In our research, the abnormal grain growth may occur from the excess 0.5 wt% PbO in the mixture and from the Pb-source ($PbZrO_3$) during the sintering step. The fractured samples (Figure 5(b) and 5(d)) showed the mix of inter- and trans-granular fracture characteristics. Villegas *et al*. (1999) reported that the inter-granular fracture appeared from the covering of a PbO-rich layer on the grain as a result of the weakness at the grain boundaries. On the other hand, when some grains were not covered with a PbO layer, the fracture illustrated the trans-granular type.

Physical Properties

The physical properties of the ceramics from HBM and CBM sintered at 1100°C for 2 h are displayed in Table 2. The PbO loss of the sintered ceramics from CBM was shown to be higher than that of the ceramics from HBM. Generally, the amount of PbO loss always depended upon the excess PbO added into the system (Costa *et al*., 2001). Therefore, the amount of excess PbO in PMN-PT had to be limited because the PbO liquid phase at the grain boundaries could contribute to the PbO loss and then generate the porosity. However, the density of the sintered ceramics from HBM was slightly higher than that of the sintered ceramics from CBM because the ceramics from HBM had more shrinkage as well as less porosity compared with the ceramics from CBM as shown in Figure 5(b) and 5(d).

Electrical Properties

The results of the electrical properties on the sintered 0.65PMN-0.35PT ceramics prepared from HBM- and CBM-derived powders are described in Table 3. The electrical properties of the ceramics from the HBM-derived powder were significantly higher than those of ceramics from the CBM-derived powder. This was because the ceramics from the HBM-derived powder yielded a higher relative density resulting in more efficiency of polarization orientation during the poling process. This could improve the electrical properties of the ceramics from

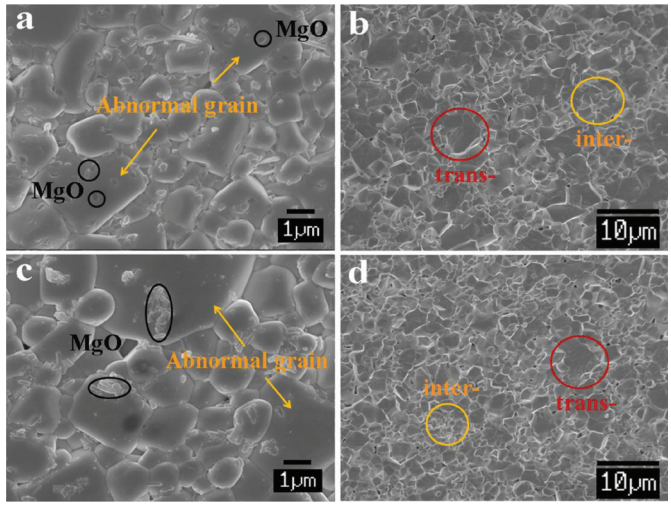

Figure 5. SEM micrographs of surface and fracture of the sintered ceramics from (a-b) HBM calcined powders and (c-d) CBM calcined powders

Table 2. Physical properties of 0.65PMN-0.35PT ceramics from HBM and CBM sintered at 1100°C for 2 h

Method	PbO loss (%)	Shrinkage (%)	Relative density (%)
HBM	0.43 ± 0.29	15.90 ± 0.13	96.6
CBM	0.83 ± 0.04	12.66 ± 0.11	95.9

Table 3. Electrical properties of 0.65PMN-0.35PT ceramics from HBM- and CBM-derived powders sintered at 1100°C for 2 h

Method	d_{33} (pC/N)	K	Tan δ	k_p	k_t
HBM	516	4066	0.0136	0.62	0.46
CBM	390	3337	0.0085	0.49	0.39

Measured at 1 kHz at room temperature

HBM-derived powder which possessed the d_{33} = 516 pC/N, k_p =0.62, and k_t = 0.46. Nevertheless, the ceramics prepared from the CBM-derived powder may require a higher sintering temperature to improve their density due to their lower sinterability. This will subsequently improve the electrical properties of the piezoelectric ceramics as mentioned in previous research (Kong *et al*., 2008).

Conclusions

The high-energy ball milling technique was successfully used to grind PMN-PT to a submicron range powder. As a result, a powder with high sinterability was obtained. It was obviously seen that the PMN-PT ceramics could be sintered at 1100°C for 2 h which is lower than the ordinary PMN-PT ceramic (sintering temperature at 1200-1250°C). The electrical properties of ceremics from the HBM-derived powder showed the d_{33} of 516 pC/N, K of 4066, k_p of 0.62, and k_t of 0.46. The high-energy ball milling technique is a promising method and alternative route to synthesize PMN-PT powder.

Acknowledgements

This research was supported by the Thailand Institute of Scientific and Technological Research (TISTR).

References

Amorin, H., Ricote, J., Holc, J., Kosec, M., and Alguero, M., (2008). Homogeneous template grain growth 0.65Pb($Mg_{1/3}Nb_{2/3}$)O3-0.35$PbTiO_3$ from nanocrytalline powders obtained by mechanochemical activation. J. Eur. Ceram. Soc., 28:2755-2763.

Brankovic, Z., Brankovic, G., Jovalekic, C., Manietta, Y., Cilense, M., and Varela, J.A. (2003). Mechanochemical synthesis of PZT powders. Mater. Sci. Eng. A., 345:243-248.

Costa, A.L., Galassi, C., Fabbri, G., Roncari, E., and Capiani, C. (2001). Pyrochlore phase and microstructure development in lead magnesium niobate materials. J. Eur. Ceram. Soc., 21:1165-1170.

Gorzkowshi, E.P., Chan, H.M., and Harmer, M.P. (2006). Effect of PbO on the kinetic of {001} Pb($Mg_{1/3}Nb_{2/3}$)O_3-35 mol% $PbTiO_3$ single crystals grown into fully dense matrices. J. Am. Ceram. Soc., 89:856-862.

Haertling, G.H. (1999). Ferroelectric ceramics: history and technology. J. Am. Ceram. Soc., 82:797-817.

Kelly, J. (1998). A study of electromechanical properties of PMN-PT ceramics and analysis of the effects of loss on frequency response of piezoelectric ceramics, [Ph.D. thesis]. Rutgers University, New Brunswick, NJ, USA.

Kelly, J., Farrey, G., and Safari, A. (1996). A comparision of the properties of (1-x)PMN-xPT ceramics near the morphotropic phase boundary prepared by sol-gel and columbite precursor methods. Proceedings of the Tenth IEEE International Symposium on the Application of Ferroelectrics; August 18-21, 1996; East Brunswick, NJ, USA, p. 699-702.

Klug, H.P. and Alexander, L.E. (1974). X-ray Diffraction Procedures, 2nd ed. Wiley, NY, USA, 992p.

Kong, L.B., Zhang, T.S., Ma, J., and Boey, F. (2008). Progress in synthesis of ferroelectric ceramic materials via high-energy mechanochemical technique. Prog. Mater. Sci., 53:207-322.

Ng, S.N., Tan, Y.P., and Taufig-Yap Y.H. (2009). Mechanochemical synthesis and characterization of bismuth-niobium oxide ion conductors. J. Phys. Sci., 20(1):75-86.

Swart, S.L. and Shrout, T.R. (1982). Fabrication of perovskite lead magnesium niobate. Mater. Res. Bull., 17:1245-1250.

Villegas, M., Fernandez, J.F., and Caballero, A.C. (1999). Effect of PbO excess in $Pb(Mg_{1/3}Nb_{2/3})O_3$-$PbTiO_3$ ceramics: Part II. Microstructure development. J. Mater. Res., 14:898-902.

Wongmaneerung, R., Sarakonsiri, T., Yimnirun, R., and Anata, S. (2006). Effects of magnesium niobate precursor and calcinations condition on phase formation and morphology of lead magnesium niobate powders. Mater. Sci. Eng. B., 132:292-299.